One Stone with Two Birds: A Null-Text-Null Frequency-Aware Diffusion Models for Text-Guided Image Inpainting

Haipeng Liu[†] **Yang Wang**[†][*] **Meng Wang**
School of Computer Science and Information Engineering
Hefei University of Technology, China
hpliu_hfut@hotmail.com yangwang@hfut.edu.cn eric.mengwang@gmail.com

Abstract

Text-guided image inpainting aims at reconstructing the masked regions as per text prompts, where the longstanding challenges lie in the preservation for unmasked regions, while achieving the semantics consistency between unmasked and inpainted masked regions. Previous arts failed to address both of them, always with either of them to be remedied. Such facts, as we observed, stem from the entanglement of the hybrid (e.g., mid-and-low) frequency bands that encode varied image properties, which exhibit different robustness to text prompts during the denoising process. In this paper, we propose a null-text-null frequency-aware diffusion models, dubbed **NTN-Diff**, for text-guided image inpainting, by decomposing the semantics consistency across masked and unmasked regions into the consistencies as per each frequency band, while preserving the unmasked regions, to circumvent two challenges in a row. Based on the diffusion process, we further divide the denoising process into early (high-level noise) and late (low-level noise) stages, where the mid-and-low frequency bands are disentangled during the denoising process. As observed, the stable mid-frequency band is progressively denoised to be semantically aligned during text-guided denoising process, which, meanwhile, serves as the guidance to the null-text denoising process to denoise low-frequency band for the masked regions, followed by a subsequent text-guided denoising process at late stage, to achieve the semantics consistency for mid-and-low frequency bands across masked and unmasked regions, while preserve the unmasked regions. Extensive experiments validate the superiority of NTN-Diff over the state-of-the-art diffusion models to text-guided diffusion models. Our code can be accessed from `https://github.com/htyjers/NTN-Diff`.

1 Introduction

Traditional image inpainting methods [23, 24, 3, 41, 46, 16, 19] primarily rely on unmasked regions as guidance to recover masked areas, which are widely applied to object removal [18, 45, 28] and photo restoration [21, 2, 27]. Based on that, text-guided image inpainting [1, 35, 47, 4, 36, 17] has achieved remarkable progress, offering a more flexible and diverse approach. These methods focus on reconstructing user-specified objects within masked regions given text prompts.

The success of text-guided image inpainting is largely attributed to the powerful generative capabilities of Denoising Diffusion Probabilistic Models (DDPMs) [9], *e.g.*, Stable Diffusion [33]. As a critical

[†] Equal contribution
[*] Yang Wang is the corresponding author

39th Conference on Neural Information Processing Systems (NeurIPS 2025).

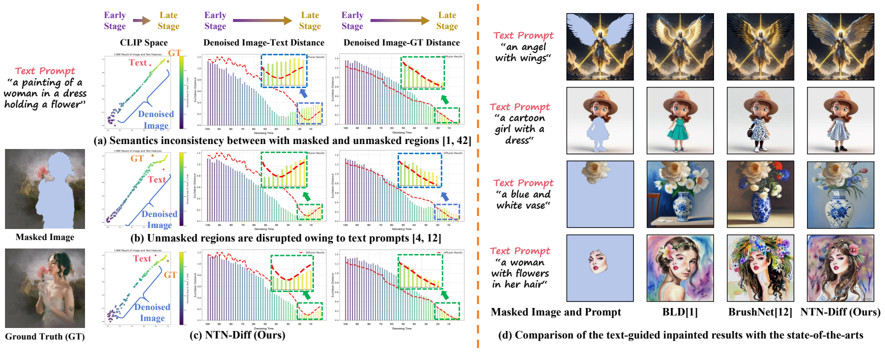

(a) Semantics inconsistency between with masked and unmasked regions [1, 42]

(b) Unmasked regions are disrupted owing to text prompts [4, 12]

(c) NTN-Diff (Ours)

(d) Comparison of the text-guided inpainted results with the state-of-the-arts

Figure 1: (a-c) t-SNE visualization of CLIP latent space evolution during text-guided denoising. At each step, the Euclidean distance between the text prompt and the denoised image (Denoised Image-Text Distance) reflects semantic consistency across masked and unmasked regions—a smaller value indicates better alignment. As a reference, we include the distance between the ground truth and the text prompt (red dashed line). To assess unmasked region preservation, we also compute the distance between the denoised image and ground truth (Denoised Image-GT Distance). (d) Comparison between our NTN-Diff (Fig.3) and state-of-the-arts [1, 12] for text-guided inpainting;

subtask in the broader field of image editing [20, 8, 7, 11, 15, 22], text-guided image inpainting distinguishes itself from other subtasks by requiring the masked regions to be generated as per text prompt, while preserve the unmasked regions. Upon the alignment between the generated content for masked regions and the text prompts, the longstanding challenges lie in *the preservation for unmasked regions, while achieving the semantics consistency between unmasked and masked regions as inpainted.*

To circumvent the above two challenges, a series of text-guided diffusion models [42, 25, 1, 35] have been proposed for image inpainting. Specifically, BLD [1] implements a blending operation during the denoising process at each step to preserve the unmasked regions, while Smartbrush [42] adopts a multi-task based denoising process conditioned on both text and shape for each step, where the denoised unmasked region is substituted by unmasked regions from ground-truth. Despite the unmasked preservation, as illustrated in Fig.1(a), they still suffer from *the semantics inconsistency between with masked and unmasked regions*, owing to the discrepancy from the *diffusion* process and the inpainted maksed regions from the *text-guided denoising* process.

Orthogonally, great efforts have been spent [31, 47, 4, 17, 26, 49] on preserving the unmasked regions while ensuring the semantics consistency between masked and unmasked regions. For instance, CAT [4] utilizes the text prompts and unmasked regions in the CLIP latent space to form latent code-level semantics consistency constraints for image inpainting, which, however, suffer from the information loss for unmasked regions. BrushNet [12] generates dense texture feature map during the denoising process with no cross-attention in UNet [34], to inpaint masked regions by unmasked information for consistency. However, as illustrated in Fig.1(b), *the unmasked regions fail to be preserved*, which is incurred by the other text-guided denoising process to inpaint masked regions.

So far, the prior arts still fail to *simultaneously* overcome the above two challenges. Such failure, as investigated in Fig.2, stems from the following hurdle: as disclosed by [29], the low-frequency band fluctuates more significantly during the early stage of the denoising process with high-level noise than the mid-and-high frequency bands, since diffusion models typically recover the low-frequency band first and progressively refine the mid-and-high frequency bands[1](***See more results in Sec.A of the Appendix***). Therefore, the *low-frequency* band for both masked and unmasked regions are easy to be modulated by text prompts, as illustrated in Fig.2(a). To be contrary, as seen in Fig.2(b), the *mid-frequency* band across all regions is robust to the text prompts while aligns well with text prompts, which may better preserve the unmasked regions than low-frequency band upon text prompts. The above observations further motivate us to decompose the semantics consistency across masked and unmasked regions into the individual task of achieving that as per each frequency band across masked

[1] Compared to the mid-frequency band, the high-frequency band is sparser and more easy to be disrupted by high-level noise in the early stages, resulting in much less contribution on guiding the low-frequency band than mid-frequency band. Therefore, we focus on mid-and-low frequency bands.

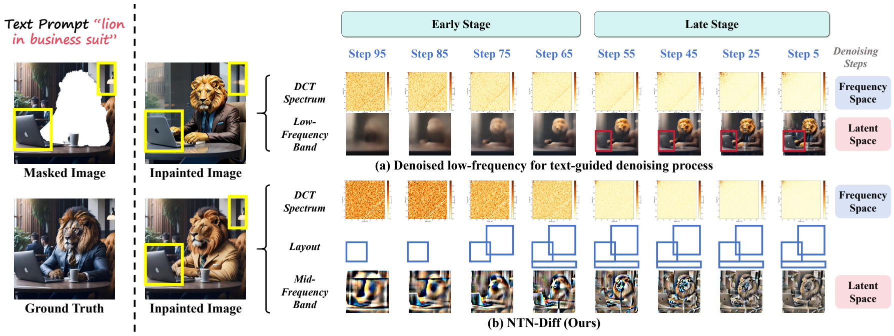

(a) Denoised low-frequency for text-guided denoising process

(b) NTN-Diff (Ours)

Figure 2: We investigate the text-guided denoising process for both the (a) low-frequency and (b) mid-frequency bands. For each step, we employ the red bounding boxes to highlight the variations for the low-frequency band during the late stage in (a) and the blue bounding boxes to visualize the variations for layout information in (b). For DCT spectrum, the top-left region represents low frequencies, with the bottom-right region corresponds to high frequencies. The dark red and yellow indicate the highest and lowest value.

and unmasked regions, while preserving the unmasked regions, to tackle two challenges in a row. To this end, we formally delve into the following questions: How to disentangle different frequency bands, particularly the *early* stage of the denoising process with high-level noise? and How to exploit the hybrid frequency bands for diffusion models to simultaneously achieve the above two goals?

Inspired by the recent progress on frequency-domain based diffusion models [39, 14, 10], we answer the above questions by proposing a frequency-aware null-text-null diffusion models, named NTN-Diff (see Fig.3), which comprises *early* and *late* stages for text-guided image inpainting. For the *early* stage, 1) we first propose a *null-text denoising process* (Sec.2.3.1) to avoid the low-frequency band is influenced by text prompts under the high-level noise, then replace its denoised result with unmasked regions from the forward diffused results. In parallel, 2) we perform the second *text-guided denoising process* (Sec.2.3.2) to denoise the masked regions, especially its mid-frequency band to be aligned with text prompts across both masked and unmasked regions, while replace the low-frequency band from the denoised output with that from the above null-text denoising process, so that the low-frequency can be preserved without being disturbed by text prompts; 3) we further exploit the above denoised mid-frequency to guide the last *null-text denoising process* (Sec.2.3.3), by substituting mid-frequency band from this null-text denoising process, while denoising the low-frequency band especially for masked regions, to attempt the complete alignment with text prompts.

Based on the above, during the *late* stage, we perform the *text-guided denoising process* (Sec.2.4), together with the unmasked regions substitution from the *early* stage of the diffusion process for unmasked regions preservations for each step, while achieve the semantics consistency between mid-and-low frequency bands across both masked and unmasked regions conditioned on text prompts, to well resolve the two challenges, leading to final inpainted output in Fig.1(c). Fig.1(d) further validates the intuition of NTN-Diff, which not only can achieve better semantics consistency between masked and unmasked regions than BLD [1], but also preserves the unmasked regions to outperform BrushNet [12], upon the alignment with text prompts.

The above observations further validate the intuitions of NTN-Diff by resolving the above two challenges, *i.e.*, semantics consistency between masked and unmasked regions and unmasked regions preservation, for the text-guided image inpainting via diffusion models. The extensive experimental results validate its superiority over the state-of-the-arts for text-guided image inpainting.

2 Methodology

Central to our proposed NTN-Diff lies in the following aspects: 1) the motivation of hybrid frequency aware diffusion models to text-guided image inpainting (Sec.2.2); 2) how to disentangle different frequency bands and exploit the hybrid frequency bands for diffusion models in the early stage (Sec.2.3); 3) how to achieve unmasked regions preservation and semantics consistency with masked regions in the late stage (Sec.2.4); before shedding light on NTN-Diff, we elaborate the preliminaries regarding DDPMs, which plays a pivotal role of text-guided image inpainting.

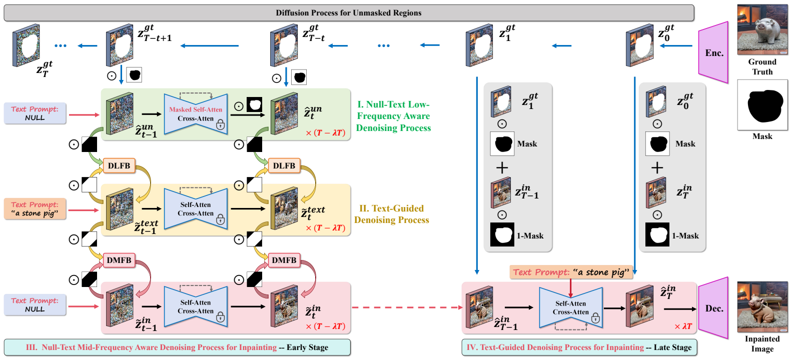

Figure 3: Illustration of our proposed NTN-Diff pipeline, which comprises a (I) *null-text denoising process* (Sec.2.3.1) to avoid being influenced by text prompts, and a (II) *text-guided denoising process* (Sec.2.3.2) to denoise the masked regions, while replacing the low-frequency band from the denoised output with that from the above null-text denoising process. Building on this, we further utilize the denoised mid-frequency to guide another (III) *null-text denoising process* (Sec.2.3.3) by substituting the mid-frequency band from this process. Additionally, a (IV) late-stage text-guided denoising process (Sec.2.4) is performed, along with the substitution of unmasked regions from the early stage of the diffusion process, to preserve unmasked regions at each step.

2.1 Preliminaries

Given a completed image $I_{gt} \in \mathbb{R}^{3\times H\times W}$, a text prompt c, and a binary mask $M \in \{0,1\}^{1\times H\times W}$ such that 0 denotes masked regions and 1 denotes unmasked regions, The goal of text-guided image inpainting is to restore the missing regions in a masked image $I_m = I_{gt} \odot M$, so that the reconstructed content aligns with the text prompts to precisely indicate *where* and *what* to be inpainted. To this end, state-of-the-arts predominantly leverage pre-trained text-to-image latent diffusion frameworks, mainly for Stable Diffusion [33] (SD) as their foundation, where Variational Auto-Encoder (VAE) [13] is employed via encoder $\mathcal{E}$ to transform the image I_{gt} from pixel space to latent space $z^{gt} \in \mathbb{R}^{4\times \frac{H}{8}\times\frac{W}{8}}$, to reduce computational complexity without compromising visual quality. The model then performs the forward diffusion process and denoising process in the latent space:

Forward Diffusion Process. In the forward diffusion process with T timesteps, following the typical Denoising Diffusion Probabilistic Model (DDPM) [9], Stable Diffusion adds Gaussian noise $\epsilon \sim \mathcal{N}(0, I)$ to convert the clean sample $z_0 = z^{gt}$ into a noisy sample z_T. For any timestep $t \in [0, T]$, the forward process z_t is then defined as:

$$z_t(z_0, \epsilon) = \sqrt{\bar{\alpha}_t} z_0 + \sqrt{1-\bar{\alpha}_t}\epsilon, \tag{1}$$

where $\bar{\alpha}_t$ denotes the corresponding noise level.

Reverse Denoising Process. During the reverse denoising process, Stable Diffusion is trained to estimate the noise added to the noisy image, conditioned on c, and progressively removes it over T timesteps. Given an input noise z_T sampled from a random Gaussian distribution, the training objective of the denoising network (UNet [34]) ϵ_θ at the t-th timestep is formulated as:

$$\mathcal{L}_{LDM} = \mathbb{E}_{z_0,c,t\sim\mathcal{U}(0,T),\epsilon\sim\mathcal{N}(0,I)} \left\|\epsilon_\theta(z_t, t, \tau_\theta(c)) - \epsilon\right\|_2^2, \tag{2}$$

where $\tau_\theta(\cdot)$ is the CLIP [30] text encoder, and $\|\cdot\|_2$ denotes the ℓ_2 norm. After T timesteps, the denoised latent representation z'_0 is reconstructed into pixel space via the decoder $\mathcal{D}$ to generate the final result I_{gen}.

2.2 Motivation: Hybrid Frequency Aware Diffusion Models to Text-Guided Image Inpainting

Before shedding light on our pipeline, upon the diffusion process as per Eq.(1), we investigate the text-guided denoising process for both the denoised *low-frequency* (dense texture [17]) and *mid-frequency* (extracted from the Discrete Cosine Transform spectrum via mid-pass mask [5, 6]) information. The compared results are shown in Fig.2, while observe the followings:

(1) As shown in Fig.2(a), the low-frequency band can be easily changed by text prompts, especially the early stage with high-level noise, such trend keeps on even into nearly the middle (*e.g.*, 45-th step) of the late stage.

(2) Fig.2(b) illustrates the text-guided denoising results for mid-frequency band. To validate its stability, we visualize the layout information as bounding box for each step (2nd row), which, as indicated by [5, 6, 43], is closely related to the mid-frequency band. Akin to Fig.2(a), the denoised mid-frequency band (3rd row) also changes during the initial early stage owing to text prompts with high-level noise, yet quickly converges by the end (*e.g.,* 65-th step) of the early stage, which further leads to the stable mid-frequency band with *nearly* no influence by text prompt across the whole late stage with low-level noise.

Capitalizing on the discoveries, instead of low-frequency, we propose to exploit the *mid-frequency* band during denoising process, which plays the pivotal role of achieving the semantics consistency upon text prompts, while can better achieve the semantics consistency between masked and unmasked regions, while preserve its own frequency band well, than low-frequency band, owing to its *robustness* to the text prompt during the denoising process. The above observations further motivate us with a novel frequency-aware null-text-null diffusion models, named NTN-Diff, for text-guided image inpainting. Our pipeline is illustrated in Fig.3, where we discuss NTN-Diff within the *early* and *late* stages, demarcated by the critical step λT with T as the total steps for diffusion models; the detailed discussions for λ can be seen in Sec.3.3.2. (***See more intuitions on hybrid frequency aware diffusion models to text-guided image inpainting in Sec.B of the Appendix***)

2.3 Early Stage for Null-Text-Null Frequency-Aware Diffusion Models

Based on the diffusion process regarding Eq.(1), we discuss the early stage of text-guided denoising process. Unlike the typical models [42, 1] with text-guided denoising process, 1) we propose a *null-text denoising process* (Sec.2.3.1) conditioned on null-text prompt at the t-th step to avoid being influenced by text prompts even under the high-level noise, focusing primarily on low-frequency band, we then replace its denoised result with the unmasked regions from the forward diffused results within the $(T-t)$-th step. In parallel, 2) we perform the second *text-guided denoising process* (Sec.2.3.2) for t-th step, to denoise the masked regions, while replace the low-frequency band (Fig.4(a)) from the denoised output with that from the above null-text denoising process, so that low-frequency band (*e.g.*, color and illumination) especially for unmasked regions can be preserved even under text prompts, while the mid-frequency band over both masked and unmasked regions varies owing to text prompts, yet struggling to be semantically consistent to its low-frequency band across the whole regions, resulting in semantic inconsistency between masked and unmasked regions (see Fig.6).

The denoised mid-frequency band well aligns with the text prompts especially for masked regions, while also encodes the information related to low-frequency band from the above null-text denoising process (Sec.2.3.3), which is further exploited to guide 3) the last *null-text denoising process*, to 3.1) achieve semantics consistency between mid-and-low frequency bands across masked and unmasked regions, by denoising the low-frequency band throughout the path to be semantically consistent to mid-frequency band, with no influence from text prompts (see Fig.2(a)); 3.2) such intuition can further restore low-frequency band especially for masked regions, to be aligned with text prompts, while ready to preserve both mid-and-low frequency bands for unmasked regions, along with its semantics consistency to masked regions via a late stage *text-guided denoising process* in Sec.2.4.

2.3.1 Null-Text Low-Frequency Aware Denoising Process

Formally, we initialize the denoising process with random Gaussian noise $z_T^{un} \in \mathbb{R}^{4\times\frac{H}{8}\times\frac{W}{8}}$ and null-text $c_\emptyset$ as the input to the denoising network $\epsilon_\theta(z_T^{un}, T, \tau_\theta(c_\emptyset))$ for *null-text denoising process*. To preserve the unmasked regions, at each step t, we replace the unmasked regions of denoising result z_t^{un} with those from the diffusion result z_{T-t}^{gt} at the $(T-t)$-th step to yield $\hat{z}_t^{un}$, as per the following:

$$\hat{z}_t^{un} = z_{T-t}^{gt} \odot m_z + z_t^{un} \odot (1 - m_z), \tag{3}$$

where $m_z \in \mathbb{R}^{1\times\frac{H}{8}\times\frac{W}{8}}$ is obtained by downsampling the mask M, we replicate it along four channels for z_{T-t}^{gt} and z_t^{un}, $\odot$ is the element-wise multiplication. Following the above, we reformulate the self-attention mechanism of the denoising network by incorporating a mask to suppress the attention scores of the masked regions, to ensure that the inpainting process primarily relies on the unmasked regions. Given the denoised latent image feature $F_l \in \mathbb{R}^{(h_l\times w_l)\times d_l}$ at the l-th layer of denoising UNet architecture $\epsilon_\theta(z_t^{un}, t, \tau_\theta(c_\emptyset))$ at the t-th timesteps, the modified self-attention mechanism is

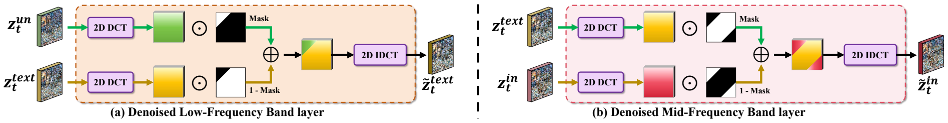

Figure 4: Illustration of (a) denoised low-frequency band layer and (b) mid-frequency band layer.

defined as follows:

$$F_{l+1} = \text{softmax}\left(\frac{\left(F_l W_{Q_l^s}\right)\left(F_l \odot m_l W_{K_l^s}\right)^T}{\sqrt{d_l}}\right) F_l W_{V_l^s}, \tag{4}$$

where $m_l \in \mathbb{R}^{h_l \times w_l}$ is the downsampled result of the mask M, we replicate it along d_l channels for F_l, $W_{Q_l^s} \in \mathbb{R}^{d_l \times d_{l+1}}$, $W_{K_l^s} \in \mathbb{R}^{d_l \times d_{l+1}}$ and $W_{V_l^s} \in \mathbb{R}^{d_l \times d_{l+1}}$ are learnable linear projection matrices, with d_l representing the embedding dimensions.

2.3.2 Text-Guided Denoising Process

To inpaint the masked regions as per text prompts, we resort to the *text-guided denoising process*, together with low-frequency band substitution from null-text denoising process (Sec.2.3.1). Specifically, we initialize the denoising process with random Gaussian noise $z_T^{text} \in \mathbb{R}^{4 \times \frac{H}{8} \times \frac{W}{8}}$ and text prompts c as the input to the denoising network $\epsilon_\theta(z_T^{text}, T, \tau_\theta(c))$ for text-guided denoising process for masked regions. As inspired by Fig.2, we preserve the unmasked regions as per their low-frequency band, since, instead of mid-frequency or even high-frequency band, such information can be easily modulated by text prompt. To this end, we propose a plug-and-play Denoised Low-Frequency Band layer (Fig.4(a)) to substitute the latent representation z_t^{text} within the text-guided denoising process, by z_t^{un} from the null-text denoising process (see Sec.2.3.1) for the t-th step to yield $\tilde{z}_t^{text}$, which is formulated as:

$$\tilde{z}_t^{text} = \text{IDCT}\left(\text{DCT}(z_t^{un}) \odot m_{low} + \text{DCT}(z_t^{text}) \odot (1 - m_{low})\right), \tag{5}$$

where DCT$(\cdot)$ represents 2D Discrete Cosine Transform, IDCT$(\cdot)$ represents 2D Inverse DCT, and m_{low} denotes the low-pass mask to isolate low-frequency band, the denoised low-frequency band layer employs a binary mask defined by the sum of the 2D coordinates as a threshold, as follows:

$$m_{low}(x, y) = \begin{cases} 1, & \text{if } x + y \leq th_{lp} \\ 0, & \text{otherwise} \end{cases} \tag{6}$$

where th_{lp} is the threshold for low-pass filtering. To adaptively extract the low-frequency band from masked images, we set th_{lp} as follows:

$$th_{lp} = \lambda_{lp}^f + \lambda_{lp}^r \cdot \frac{\|M\|_1}{HW}, \tag{7}$$

where λ_{lp}^f and λ_{lp}^r are hyper-parameters. The ℓ_1 norm $\|M\|_1$ represents the number of entry with value 1 in M. We set th_{lp} to correlate with the ratio of unmasked regions, since the larger unmasked regions require more low-frequency band from the null-text denoising process to substitute the low-frequency band within the text-guided denoising process.

Remark 1. During this process, the low-frequency band across both masked and unmasked regions are preserved even under text prompts owing to the substitutions from the null-text denoising process, with only mid-frequency aligned with text prompts for both regions, hence still failed to achieve the consistency between masked and unmasked regions. To address this, we propose another concurrent *null-text denoising process*, guided by above denoised mid-level frequency, to help denoise the low-frequency band for both regions, especially for masked regions.

2.3.3 Null-Text Mid-Frequency Aware Denoising Process

We resort to another *null-text denoising process* guided by the denoised mid-frequency band from the second text-guided denoising process (Sec.2.3.2) for the t-th step of the early stage. Particularly, we initialize the denoising process with random Gaussian noise $z_T^{in} \in \mathbb{R}^{4 \times \frac{H}{8} \times \frac{W}{8}}$ and null-text $c_\emptyset$ as input to the denoising network $\epsilon_\theta(z_T^{in}, T, \tau_\theta(c_\emptyset))$. We further exploit the denoised mid-frequency result from z_t^{text} , to substitute the denoised mid-frequency band of z_t^{in} from the last *null-text denoising* *process*, throughout a plug-and-play Denoised Mid-Frequency Band layer (as illustrated in Fig.4(b)) to yield $\tilde{z}_t^{in}$, which is formulated below:

$$\tilde{z}_t^{in} = \text{IDCT}\left(\text{DCT}(z_t^{text}) \odot m_{\text{mid}} + \text{DCT}(z_t^{in}) \odot (1 - m_{\text{mid}})\right), \tag{8}$$

where m_{mid} denotes the mid-pass mask. Analogous to Eq. (6), we define:

$$m_{\text{mid}}(x, y) = \begin{cases} 1, & \text{if } th_{mp1} < x + y \leq th_{mp2} \\ 0, & \text{otherwise} \end{cases} \tag{9}$$

where th_{mp1} and th_{mp2} are the thresholds for mid-pass filtering to extract mid-frequency band. To adaptively extract the mid-frequency band from masked images, we set th_{mp1} and th_{mp2} as follows:

$$th_{mp1} = \lambda_{mp1}^f - \lambda_{mp1}^r \cdot \frac{\|M\|_1}{HW}, th_{mp2} = \lambda_{mp2}^f + \lambda_{mp2}^r \cdot \frac{\|M\|_1}{HW}, \tag{10}$$

where λ_{mp1}^f, λ_{mp1}^r, λ_{mp2}^f and λ_{mp2}^r are hyper-parameters, such that $th_{mp2} > th_{mp1}$. Similar as Eq. (7), we also set the th_{mp1} and th_{mp2} to correlate with the ratio of unmasked regions. Since the larger unmasked regions require more mid-frequency band to encode the information from the low-frequency band substituted from the first null-text denoising process.

Remark 2. The above null-text mid-frequency guided denoised process can denoise the low-frequency band for the masked regions to be aligned with text prompt, owing to *the denoised mid-frequency from text-guided process*; besides, the denoised mid-and-low frequency bands from unmasked regions also help denoising process for masked regions, which, however, cannot be served as the final text-guided inpainting output for masked regions, as the denoised mid-and-low frequency band is not semantically strong as text prompt. To address that, a *text-guided denoising process* is performed as the late stage of denoising process, as discussed below.

2.4 Late Stage of Text-Guided Denoising Process

Following the discussion above, for final late stage of denoising process, we perform the *text-guided denoising process* based on the early null-text mid-frequency guided denoising process (Sec.2.3.3), the low-frequency band within the masked regions is denoised throughout the path to text prompts alignment, together with the stable mid-frequency band (see Fig.2(b)) from the early text-guided denoising process (Sec.2.3.2), the masked regions are well inpainted. However, the low-frequency band for unmasked regions biases a lot from the ground truth from the early null-text denoising process (Sec.2.3.3), and augmented by the influence from the text prompts for late stage. To this end, we substitute the unmasked regions from early stage of the diffusion process into the denoising results z_t^{in} for the t-th step during the late stage to yield $\hat{z}_t^{in}$, which is formulated as:

$$\hat{z}_t^{in} = z_{T-t}^{gt} \odot m_z + z_t^{in} \odot (1 - m_z), \tag{11}$$

where z_{T-t}^{gt} donates the forward diffused results with the $(T-t)$-th step. Building upon the noisy sample $\hat{z}_t^{in}$, the text prompt c, along with the step t, we perform the denoising network $\epsilon_\theta(\hat{z}_t^{in}, t, \tau_\theta(c))$ to get the denoising result z_{t-1}^{in} in the latent space for the next $(t-1)$-th step. After λT steps, the denoised latent representation z_0^{in} is reconstructed into the pixel space via the VAE decoder $\mathcal{D}$ to generate the final image inpainting output. (***See the pseudo algorithm in Sec.C of the Appendix***)

Remark 3 : Last question on Semantics Consistency is answered! Although the alignment between mid-and-low frequency bands from masked regions and text prompts, together with unmasked regions preservation, can be achieved, one last question is *how the denoised results within this late stage can achieve semantics consistency between masked and unmasked regions?* The crucial intuition lies in the denoised mid-frequency band from the early text-guided denoising process (Sec.2.3.2), which, based on **Remark 2**, also encodes the information from the low-frequency band substituted from the null-text denoising process to match diffusion process (ground truth) including both masked and unmasked regions, hence the low-frequency band under mid-frequency guidance for masked regions also achieves the consistency to the substituted unmasked regions from the diffusion process, since the mid-frequency band is *stable* during the late stage of the denosing process *even under text prompts* (see Fig.2(b)).

With all frequency bands to be semantically consistent across all regions conditioned on text prompts, the *semantics consistency* between masked and unmasked are well achieved, together with the success of the *preservation for unmasked regions*!

Table 1: Quantitative comparisons between NTN-Diff (*) and other diffusion-based inpainting models over BrushBench for inpainting and outpainting are shown, where all models use **Stable Diffusion V1.5** as the baseline model. ↑: higher is better; ↓: lower is better; **red** and **blue** stand for the best and second best result. * with blending operation of BrushNet. NTN-Diff (*) achieves the best result.

Metrics			Image Quality		Masked Region Preservation			Text Align
Task	**Models**	**Venue**	**IR**$_{\times 10}$↑	**HPS v2**$_{\times 10^2}$↑	**PSNR**↑	**MSE**$_{\times 10^3}$↓	**LPIPS**$_{\times 10^3}$↓	**CLIP Score**↑
Inside Inpainting	**BLD**[1]	TOG' 23	9.78	25.87	21.33	9.76	49.26	26.15
	CNI[47]	ICCV' 23	9.9	26.02	12.39	78.78	243.62	26.47
	PP[49]	ECCV' 24	11.46	27.35	21.43	32.73	48.43	**26.48**
	BrushNet[12]	ECCV' 24	**12.36**	**27.40**	21.65	**9.31**	48.28	**26.48**
	HDP[25]	ICLR' 25	11.68	26.90	**22.61**	9.95	**43.50**	26.37
	NTN-Diff (Ours)	-	**12.45**	**27.57**	**23.51**	**6.50**	**40.79**	**26.54**
	CNI*[47]	ICCV' 23	11.21	26.92	22.73	24.58	43.49	26.22
	BrushNet*[12]	ECCV' 24	**12.64**	**27.78**	**31.94**	**0.80**	**18.67**	**26.39**
	NTN-Diff* (Ours)	-	**12.69**	**27.82**	**40.70**	**0.11**	**0.88**	**26.49**
Outside Inpainting	**BLD**[1]	TOG' 23	7.81	26.77	15.85	35.86	21.40	26.73
	CNI[47]	ICCV' 23	9.26	27.68	11.91	83.03	58.16	27.29
	PP[49]	ECCV' 24	7.45	28.01	18.04	31.78	15.13	26.72
	BrushNet[12]	ECCV' 24	**10.82**	**28.02**	**18.06**	22.86	**15.08**	**27.33**
	HDP[25]	ICLR' 25	9.66	27.79	18.03	22.99	15.22	26.96
	NTN-Diff (Ours)	-	**11.54**	**28.22**	**18.47**	**20.44**	**14.46**	**27.54**
	CNI*[47]	ICCV' 23	9.57	27.76	17.50	37.72	19.95	26.92
	BrushNet*[12]	ECCV' 24	**10.88**	**28.09**	**27.82**	**2.25**	**4.63**	**27.22**
	NTN-Diff* (Ours)	-	**11.61**	**28.36**	**31.08**	**1.23**	**1.24**	**27.30**

3 Experiments

3.1 Implementation Details

We evaluate NTN-Diff on two benchmarks tailored for text-guided image inpainting in diffusion models: **BrushBench** [12] comprises 600 images with human-annotated masks and captions. The dataset balances natural and artificial images (*e.g.*, paintings) and equally distributes across categories (humans, animals, indoor/outdoor scenarios), ensuring fair and equitable evaluation, BrushBench refines the task by considering two specific scenarios: segmentation mask inside-inpainting and segmentation mask outside-inpainting; **EditBench** [35] features 240 images with an equal split between natural and generated images, each accompanied by mask and caption annotations. Following [12], we utilize a fine-tuned version of **Stable Diffusion v1.5** as the base model, configured with 100 sampling steps to ensure high-quality outputs. All experiments are implemented in PyTorch and run on a single NVIDIA RTX 3090.

We evaluate inpainted results using six metrics across three aspects. For ***image generation quality***, we employ **Image Reward (IR)** [44] to model human preferences for image quality and **HPS V2** [40] that combines perceptual studies with deep learning for comprehensive visual and semantic assessment. Both metrics measure the *semantics consistency* of the high-quality image generation aligned with human standards; for ***masked region preservation***, we use **PSNR** and **MSE** to measure pixel-wise differences from ground truth, along with **LPIPS** [48] which evaluates perceptual similarity through deep feature distances; finally, for ***text alignment***, **CLIP Score** [38] quantifies *text-image consistency* by comparing their embeddings in CLIP's shared space.

3.2 Comparison with State-of-the-arts

To validate the superiority of **NTN-Diff**, we conduct a comprehensive comparison with state-of-the-art text-guided image inpainting diffusion models, including **HDP** [25] and **BLD** [1] which implement a blending operation during the denoising process at each step to preserve the unmasked regions, while suffer from the semantics inconsistency between with masked and unmasked regions, owing to the discrepancy between the diffusion process for unmasked regions substitution and the denoising process for masked region alignment with text prompt. **CNI** [47], **PP** [49] and **BrushNet** [12] focus on the ensuring the semantics consistency between masked and unmasked regions. Particularly, **BrushNet** [12] generates dense texture feature map during the denoising process with no cross-attention in UNet [34], to inpaint masked regions by unmasked information for consistency, while unmasked regions are disrupted owing to another text-guided denoising process.

Quantitative and Qualitative analysis. The quantitative results in Table.1 summarize our findings below: **NTN-Diff** enjoys larger IR, HPS v2, PSNR and CLIP Score, together with smaller MSE and LPIPS than the competitors. Notably, **BrushNet** remains the large performance margins (at most 0.73% for IR, 0.62% for HPS, 8.59% for PSNR, 30.18% for MSE, 15.51% for LPIPS and 0.23% for CLIP Score) compared to **NTN-Diff** in Table.1. We also present the quantitative results of **NTN-Diff** with the pixel-level blending operation of [12], named **NTN-Diff***, to preserve the unmasked regions,

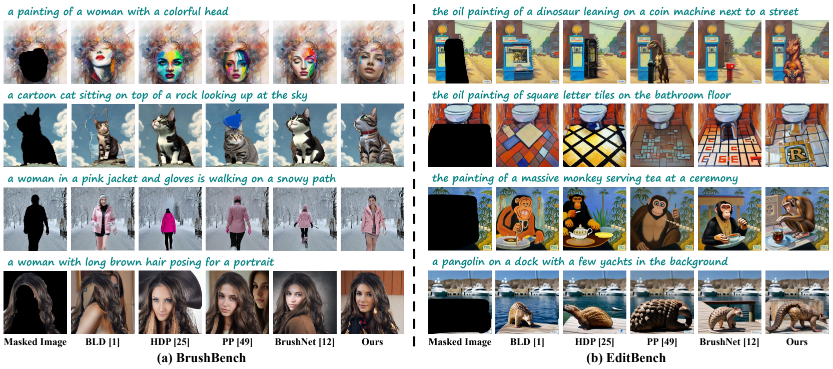
a painting of a woman with a colorful head
a cartoon cat sitting on top of a rock looking up at the sky
a woman in a pink jacket and gloves is walking on a snowy path
a woman with long brown hair posing for a portrait
the oil painting of a dinosaur leaning on a coin machine next to a street
the oil painting of square letter tiles on the bathroom floor
the painting of a massive monkey serving tea at a ceremony
a pangolin on a dock with a few yachts in the background
Masked Image
BLD [1]
HDP [25]
PP [49]
BrushNet [12]
Ours

(a) BrushBench (b) EditBench

Figure 5: Comparison of the text-guided inpainted results with the state-of-the-arts on BrushBench [12] and EditBench [35]. NTN-Diff delivers the superior inpainted results over others.

Table 2: Ablation studies on three denoising processes: Case A (Sec.2.3.1), Case B (Sec.2.3.2) and Case C (Sec.2.3.3) for the early stage, based on the same text-guided denoising process (Sec.2.4) for the late stage. **red** and **blue** stand for the best and second best result.

Metric	EditBench				BrushBench			
	Case A	Case B	Case C	**Ours**	Case A	Case B	Case C	**Ours**
IR$_{\times 10}$↑	2.41	1.24	2.14	3.10	10.14	9.59	10.02	11.12
PSNR↑	22.36	22.39	22.53	22.65	28.02	27.71	28.06	28.10
LPIPS$_{\times 10^3}$↓	26.60	24.82	25.24	24.21	44.54	47.08	44.92	44.09
CLIP Score↑	28.62	28.53	28.60	28.95	25.95	25.78	26.03	26.09

Table 3: Ablation study about the hyperparameter sensitivity analysis of λ. **red** and **blue** stand for the best and second best result. With $\lambda = 0.6$ balancing early and late stage, the best performance of image quality, unmasked region preservation and text alignment are achieved.

Metric	EditBench					BrushBench				
	0.9	0.8	0.7	0.6	0.5	0.9	0.8	0.7	0.6	0.5
IR$_{\times 10}$↑	2.41	2.67	2.78	3.10	1.10	10.56	10.40	10.76	11.12	10.77
PSNR↑	22.03	22.19	22.44	22.65	22.63	27.69	27.86	28.04	28.10	28.08
LPIPS$_{\times 10^3}$↓	30.10	29.28	26.95	24.21	23.16	49.26	46.85	44.88	44.09	43.44
CLIP Score↑	28.89	28.76	29.20	28.95	28.81	25.87	26.01	25.93	26.09	25.91

which demonstrates the ability to tame the hybrid frequency issue, the results further verifies the intuition in Sec.1 – NTN-Diff achieves the *semantics consistency* between mid-and-low frequency bands across masked and unmasked regions, while *preserving unmasked regions*. We illustrate the above intuitions in Fig.5. (***See more analysis of computational efficiency in Sec.D of the Appendix, along with more compared results for Editbench [35] can be seen in Sec.E of the Appendix***)

3.3 Ablation Studies

3.3.1 Discussion on Different Denoising Processes of the Early Stage

To validate of our NTN-Diff (Sec.2.3), we perform the ablation study on BrushBench and EditBench datasets with three variants: **Case A**: removing masked self-attention in the first null-text denoising process (Sec.2.3.1); **Case B**: removing both null-text and text-guided denoising process (Sec.2.3.2). **Case C**: removing the null-text denoising process (Sec.2.3.3); Table.2 reports the results for all three cases, which suggests that NTN-Diff outperforms **Case A**, confirming that *the null-text denoising process conditioned on null-text prompt can avoid being influenced by text prompts even under the high-level noise, focusing primarily on low-frequency band,* which in line with Sec.2.3.1; **Case B** exhibits a suboptimal performance degradation, despite the null-text denoising process in the early stage, together with the text-guided denoising process, which verifies that the null-text mid-frequency guided denoised process can denoise the low-frequency band for the masked regions to be aligned with text prompt, owing to *the denoised mid-frequency from text-guided process*, hence validating the important of text-guided process (Sec.2.3.2); NTN-Diff maintains achieves the large performance gain over **Case C** (at most 44.8%), implying that only mid-frequency *aligned with text prompts for masked and unmasked regions*, still failed to achieve the consistency across the whole regions, which is in line with Sec.2.3.3 and illustrated in Fig.6. (***See more generation results for the impact of the text and null-text prompts on low-and-mid frequency bands in Sec.F of the Appendix***).

3.3.2 Hyperparameter Sensitivity Analysis of λ for the Length of the Early and Late Stage

We analyze the parameter λ (Sec.2.2) that divides the denoising process into *early* and *late* stages at step λT, we set the λ values to $\{0.9; 0.8; 0.7; 0.6; 0.5\}$. As reported in Table.3, when $\lambda = 0.9$, the performance is the worst with the shortest early stage. When $\lambda = 0.6$ with the balance of early and late stage, the best performance are achieved, confirming that the desirable length of early stage

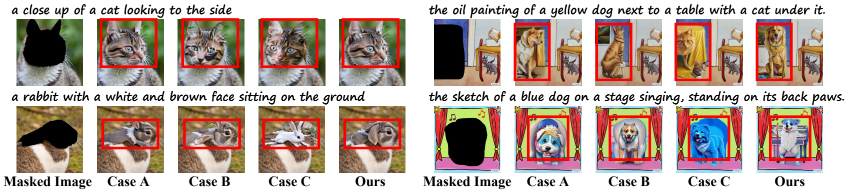
a close up of a cat looking to the side
the oil painting of a yellow dog next to a table with a cat under it.
a rabbit with a white and brown face sitting on the ground
the sketch of a blue dog on a stage singing, standing on its back paws.
Masked Image
Case A
Case B
Case C
Ours
Masked Image
Case A
Case B
Case C
Ours

Figure 6: The inpainted output about the different denoising process for the early stage, NTN-Diff delivers the better inpainted results (marked as the red box) than others. **Case A** fails to preserve the unmasked region in the null-text denoising process (Sec.2.3.1), such as the background of dog (4th row); without text-guided denoising process (Sec.2.3.2), **Case B** cannot inpaint the masked region as per the text prompts, such as the disappeared dog in the 3rd row of Case B; specifically, **Case C** cannot achieve the semantics consistency between masked and unmasked region, owing to the null-text denoising process (Sec.2.3.3), such as the tiny rabbit within the rabbit head-shaped mask.

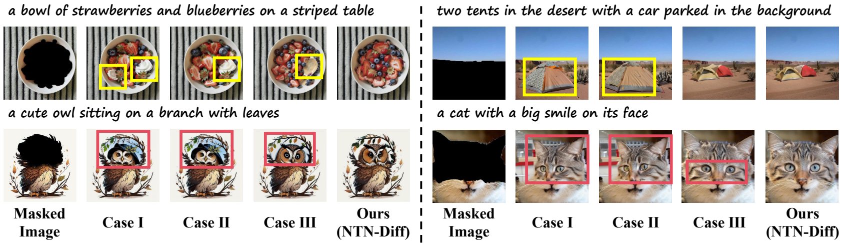
a bowl of strawberries and blueberries on a striped table
two tents in the desert with a car parked in the background
a cute owl sitting on a branch with leaves
a cat with a big smile on its face
Masked Image
Case I
Case II
Case III
Ours (NTN-Diff)
Masked Image
Case I
Case II
Case III
Ours (NTN-Diff)

Figure 7: The inpainted output about the impact of adaptively extracting the low-and-mid frequency bands, NTN-Diff can achieve the better inpainted results (marked as the **box**) than others.

can make the *low-frequency* band under the *mid-frequency guidance* for masked regions *achieve the consistency* to the substituted unmasked regions for ground truth, which is consistent to Sec.2.4. (***See more generation results in Sec.G of the Appendix***).

3.3.3 More Ablation Studies on the Impact of Adaptively Extracting the Low-and-Mid Frequency Bands

As mentioned in Sec.2.3.2 and Sec.2.3.3, we set th_{lp} in Eq.(5), and th_{mp1} and th_{mp2} in Eq.(8 to correlate with the ratio of unmasked regions. We provide ablation studies on the impact of adaptively extracting low-and-mid frequency bands on the BrushBench and EditBench datasets using three variants: **Case I** adopts fixed thresholds to extract both mid-and-low frequency bands for different images; **Case II** adaptively extracts low-frequency band while using fixed thresholds for mid-frequency bands; **Case III** adaptively extracts mid-frequency band while using a fixed threshold for low-frequency extraction. As shown in Fig.7, due to the use of fixed thresholds for extracting mid-frequency band, **Case I** and **Case II** inevitably generate inconsistent content between masked and unmasked regions (*e.g.*, the smiling cat in the second row of Fig. 7), which can be attributed to the fact *that the larger unmasked regions require more mid-frequency band to encode the information from the low-frequency band substituted from the first null-text denoising process*, as explained in Sec. 2.4. In contrast, **Case III** shows substantial performance degradation (e.g., the light yellow color blocks in the bowl in the first row of Fig.7), confirming *that larger unmasked regions demand more low-frequency information from the null-text denoising process to replace the low-frequency bands in the text-guided denoising process*, which is consistent with the findings in Sec.2.3.2.

4 Conclusion

In this paper, we propose a null-text-null frequency-aware diffusion models, named NTN-Diff, for text-guided image inpainting, by decomposing the semantics consistency across masked and unmasked regions into the consistencies as per each frequency band, while preserving the unmasked regions, to simultaneously address two challenges of unmasked regions preservations, along with its semantics consistency with inpainted masked regions. The extensive experimental results validate the advantages of NTN-Diff over state-of-the-art diffusion models for text-guided image inpainting.

Acknowledgments This research is supported by National Natural Science Foundation of China (U21A20470, 62172136, 72188101); Institute of Advanced Medicine and Frontier Technology (2023IHM01080), and sponsored by CCF-NetEase ThunderFire Innovation Research Funding (NO. CCF-Netease 202513); The computation is completed on the HPC Platform of Hefei University of Technology.

References

[1] Omri Avrahami, Ohad Fried, and Dani Lischinski. Blended latent diffusion. *ACM transactions on graphics (TOG)*, 42(4):1–11, 2023.

[2] Chenjie Cao, Qiaole Dong, and Yanwei Fu. Zits++: Image inpainting by improving the incremental transformer on structural priors. *IEEE Transactions on Pattern Analysis and Machine Intelligence*, 2023.

[3] Haiwei Chen and Yajie Zhao. Don't look into the dark: Latent codes for pluralistic image inpainting. In *Proceedings of the IEEE/CVF Conference on Computer Vision and Pattern Recognition*, pages 7591–7600, 2024.

[4] Yifu Chen, Jingwen Chen, Yingwei Pan, Yehao Li, Ting Yao, Zhineng Chen, and Tao Mei. Improving text-guided object inpainting with semantic pre-inpainting. In *European Conference on Computer Vision*, pages 110–126. Springer, 2024.

[5] Xiang Gao and Jiaying Liu. Fbsdiff: Plug-and-play frequency band substitution of diffusion features for highly controllable text-driven image translation. In *Proceedings of the 32nd ACM International Conference on Multimedia*, pages 4101–4109, 2024.

[6] Xiang Gao, Zhengbo Xu, Junhan Zhao, and Jiaying Liu. Frequency-controlled diffusion model for versatile text-guided image-to-image translation. In *Proceedings of the AAAI Conference on Artificial Intelligence*, volume 38, pages 1824–1832, 2024.

[7] Qin Guo and Tianwei Lin. Focus on your instruction: Fine-grained and multi-instruction image editing by attention modulation. In *Proceedings of the IEEE/CVF Conference on Computer Vision and Pattern Recognition*, pages 6986–6996, 2024.

[8] Amir Hertz, Ron Mokady, Jay Tenenbaum, Kfir Aberman, Yael Pritch, and Daniel Cohen-or. Prompt-to-prompt image editing with cross-attention control. In *The Eleventh International Conference on Learning Representations*.

[9] Jonathan Ho, Ajay Jain, and Pieter Abbeel. Denoising diffusion probabilistic models. *Advances in Neural Information Processing Systems (NIPS)*, 33:6840–6851, 2020.

[10] Linjiang Huang, Rongyao Fang, Aiping Zhang, Guanglu Song, Si Liu, Yu Liu, and Hongsheng Li. Fouriscale: A frequency perspective on training-free high-resolution image synthesis. In *European Conference on Computer Vision*, pages 196–212. Springer, 2024.

[11] Yuzhou Huang, Liangbin Xie, Xintao Wang, Ziyang Yuan, Xiaodong Cun, Yixiao Ge, Jiantao Zhou, Chao Dong, Rui Huang, Ruimao Zhang, et al. Smartedit: Exploring complex instruction-based image editing with multimodal large language models. In *Proceedings of the IEEE/CVF Conference on Computer Vision and Pattern Recognition*, pages 8362–8371, 2024.

[12] Xuan Ju, Xian Liu, Xintao Wang, Yuxuan Bian, Ying Shan, and Qiang Xu. Brushnet: A plug-and-play image inpainting model with decomposed dual-branch diffusion. In *European Conference on Computer Vision*, pages 150–168. Springer, 2024.

[13] Diederik P Kingma and Max Welling. Auto-encoding variational bayes. *arXiv preprint arXiv:1312.6114*, 2013.

[14] Gwanhyeong Koo, Sunjae Yoon, Ji Woo Hong, and Chang D Yoo. Flexiedit: Frequency-aware latent refinement for enhanced non-rigid editing. In *European Conference on Computer Vision*, pages 363–379. Springer, 2024.

[15] Shanglin Li, Bohan Zeng, Yutang Feng, Sicheng Gao, Xiuhui Liu, Jiaming Liu, Lin Li, Xu Tang, Yao Hu, Jianzhuang Liu, et al. Zone: Zero-shot instruction-guided local editing. In *Proceedings of the IEEE/CVF Conference on Computer Vision and Pattern Recognition*, pages 6254–6263, 2024.

[16] Wenbo Li, Zhe Lin, Kun Zhou, Lu Qi, Yi Wang, and Jiaya Jia. Mat: Mask-aware transformer for large hole image inpainting. In *Proceedings of the IEEE/CVF conference on computer vision and pattern recognition*, pages 10758–10768, 2022.

[17] Yaowei Li, Yuxuan Bian, Xuan Ju, Zhaoyang Zhang, Junhao Zhuang, Ying Shan, Yuexian Zou, and Qiang Xu. Brushedit: All-in-one image inpainting and editing. *arXiv preprint arXiv:2412.10316*, 2024.

[18] Haipeng Liu, Yang Wang, Biao Qian, Meng Wang, and Yong Rui. Structure matters: Tackling the semantic discrepancy in diffusion models for image inpainting. In *Proceedings of the IEEE/CVF Conference on Computer Vision and Pattern Recognition (CVPR)*, pages 8038–8047, June 2024.

[19] Haipeng Liu, Yang Wang, Meng Wang, and Yong Rui. Delving globally into texture and structure for image inpainting. In *Proceedings of the 30th ACM International Conference on Multimedia*, pages 1270–1278, 2022.

[20] Heng Liu, Guanghui Li, Mingqi Gao, Xiantong Zhen, Feng Zheng, and Yang Wang. Few-shot referring video single-and multi-object segmentation via cross-modal affinity with instance sequence matching. *International Journal of Computer Vision*, 133:5610–5628, 2025.

[21] Qiankun Liu, Yuqi Jiang, Zhentao Tan, Dongdong Chen, Ying Fu, Qi Chu, Gang Hua, and Nenghai Yu. Transformer based pluralistic image completion with reduced information loss. *IEEE Transactions on Pattern Analysis and Machine Intelligence*, 46(10):6652–6668, 2024.

[22] Jingyi Lu, Xinghui Li, and Kai Han. Regiondrag: Fast region-based image editing with diffusion models. In *European Conference on Computer Vision*, pages 231–246. Springer, 2024.

[23] Andreas Lugmayr, Martin Danelljan, Andres Romero, Fisher Yu, Radu Timofte, and Luc Van Gool. RePaint: Inpainting using denoising diffusion probabilistic models. In *Proceedings of the IEEE/CVF Conference on Computer Vision and Pattern Recognition (CVPR)*, pages 11461–11471, 2022.

[24] Ziwei Luo, Fredrik K Gustafsson, Zheng Zhao, Jens Sjölund, and Thomas B Schön. Image restoration with mean-reverting stochastic differential equations. *arXiv preprint arXiv:2301.11699*, 2023.

[25] Hayk Manukyan, Andranik Sargsyan, Barsegh Atanyan, Zhangyang Wang, Shant Navasardyan, and Humphrey Shi. Hd-painter: High-resolution and prompt-faithful text-guided image inpainting with diffusion models. *arXiv preprint arXiv:2312.14091*, 2023.

[26] Yotam Nitzan, Zongze Wu, Richard Zhang, Eli Shechtman, Daniel Cohen-Or, Taesung Park, and Michaël Gharbi. Lazy diffusion transformer for interactive image editing. In *European Conference on Computer Vision*, pages 55–72. Springer, 2024.

[27] Biao Qian, Yang Wang, Richang Hong, and Meng Wang. Adaptive data-free quantization. In *Proceedings of the IEEE/CVF Conference on Computer Vision and Pattern Recognition*, pages 7960–7968, 2023.

[28] Biao Qian, Yang Wang, Hongzhi Yin, Richang Hong, and Meng Wang. Switchable online knowledge distillation. In *European Conference on Computer Vision*, pages 449–466. Springer, 2022.

[29] Yurui Qian, Qi Cai, Yingwei Pan, Yehao Li, Ting Yao, Qibin Sun, and Tao Mei. Boosting diffusion models with moving average sampling in frequency domain. In *Proceedings of the IEEE/CVF Conference on Computer Vision and Pattern Recognition*, pages 8911–8920, 2024.

[30] Alec Radford, Jong Wook Kim, Chris Hallacy, Aditya Ramesh, Gabriel Goh, Sandhini Agarwal, Girish Sastry, Amanda Askell, Pamela Mishkin, Jack Clark, et al. Learning transferable visual models from natural language supervision. In *International conference on machine learning*, pages 8748–8763. PmLR, 2021.

[31] Yuxi Ren, Jie Wu, Yanzuo Lu, Huafeng Kuang, Xin Xia, Xionghui Wang, Qianqian Wang, Yixing Zhu, Pan Xie, Shiyin Wang, et al. Byteedit: Boost, comply and accelerate generative image editing. In *European Conference on Computer Vision*, pages 184–200. Springer, 2024.

[32] Robin Rombach, Andreas Blattmann, Dominik Lorenz, Patrick Esser, and Björn Ommer. High-resolution image synthesis with latent diffusion models. In *Proceedings of the IEEE/CVF Conference on Computer Vision and Pattern Recognition (CVPR)*, pages 10684–10695, June 2022.

[33] Robin Rombach, Andreas Blattmann, Dominik Lorenz, Patrick Esser, and Björn Ommer. High-resolution image synthesis with latent diffusion models. In *2022 IEEE/CVF Conference on Computer Vision and Pattern Recognition (CVPR)*, pages 10674–10685, 2022.

[34] Olaf Ronneberger, Philipp Fischer, and Thomas Brox. U-net: Convolutional networks for biomedical image segmentation. In *Medical image computing and computer-assisted intervention–MICCAI 2015: 18th international conference, Munich, Germany, October 5-9, 2015, proceedings, part III 18*, pages 234–241. Springer, 2015.

[35] Su Wang, Chitwan Saharia, Ceslee Montgomery, Jordi Pont-Tuset, Shai Noy, Stefano Pellegrini, Yasumasa Onoe, Sarah Laszlo, David J Fleet, Radu Soricut, et al. Imagen editor and editbench: Advancing and evaluating text-guided image inpainting. In *Proceedings of the IEEE/CVF Conference on Computer Vision and Pattern Recognition (CVPR)*, pages 18359–18369, 2023.

[36] Yang Wang, Biao Qian, Haipeng Liu, Yong Rui, and Meng Wang. Unpacking the gap box against data-free knowledge distillation. *IEEE Transactions on Pattern Analysis and Machine Intelligence*, 46(9):6280–6291, 2024.

[37] Zhou Wang, Alan C Bovik, Hamid R Sheikh, and Eero P Simoncelli. Image quality assessment: from error visibility to structural similarity. *IEEE transactions on image processing*, 13(4):600–612, 2004.

[38] Chenfei Wu, Lun Huang, Qianxi Zhang, Binyang Li, Lei Ji, Fan Yang, Guillermo Sapiro, and Nan Duan. Godiva: Generating open-domain videos from natural descriptions. *arXiv preprint arXiv:2104.14806*, 2021.

[39] Wei Wu, Qingnan Fan, Shuai Qin, Hong Gu, Ruoyu Zhao, and Antoni B Chan. Freediff: Progressive frequency truncation for image editing with diffusion models. In *European Conference on Computer Vision*, pages 194–209. Springer, 2024.

[40] Xiaoshi Wu, Yiming Hao, Keqiang Sun, Yixiong Chen, Feng Zhu, Rui Zhao, and Hongsheng Li. Human preference score v2: A solid benchmark for evaluating human preferences of text-to-image synthesis. *arXiv preprint arXiv:2306.09341*, 2023.

[41] Chaohao Xie, Shaohui Liu, Chao Li, Ming-Ming Cheng, Wangmeng Zuo, Xiao Liu, Shilei Wen, and Errui Ding. Image inpainting with learnable bidirectional attention maps. In *Proceedings of the IEEE/CVF international conference on computer vision*, pages 8858–8867, 2019.

[42] Shaoan Xie, Zhifei Zhang, Zhe Lin, Tobias Hinz, and Kun Zhang. Smartbrush: Text and shape guided object inpainting with diffusion model. In *Proceedings of the IEEE/CVF Conference on Computer Vision and Pattern Recognition (CVPR)*, pages 22428–22437, 2023.

[43] Wenbin Xie, Dehua Song, Chang Xu, Chunjing Xu, Hui Zhang, and Yunhe Wang. Learning frequency-aware dynamic network for efficient super-resolution. In *Proceedings of the IEEE/CVF International Conference on Computer Vision*, pages 4308–4317, 2021.

[44] Jiazheng Xu, Xiao Liu, Yuchen Wu, Yuxuan Tong, Qinkai Li, Ming Ding, Jie Tang, and Yuxiao Dong. Imagereward: Learning and evaluating human preferences for text-to-image generation. *Advances in Neural Information Processing Systems*, 36:15903–15935, 2023.

[45] Yongsheng Yu, Dawei Du, Libo Zhang, and Tiejian Luo. Unbiased multi-modality guidance for image inpainting. In *Computer Vision–ECCV 2022: 17th European Conference, Tel Aviv, Israel, October 23–27, 2022, Proceedings, Part XVI*, pages 668–684. Springer, 2022.

[46] Yu Zeng, Zhe Lin, Huchuan Lu, and Vishal M Patel. Cr-fill: Generative image inpainting with auxiliary contextual reconstruction. In *Proceedings of the IEEE/CVF international conference on computer vision*, pages 14164–14173, 2021.

[47] Lvmin Zhang, Anyi Rao, and Maneesh Agrawala. Adding conditional control to text-to-image diffusion models. In *Proceedings of the IEEE/CVF international conference on computer vision*, pages 3836–3847, 2023.

[48] Richard Zhang, Phillip Isola, Alexei A Efros, Eli Shechtman, and Oliver Wang. The unreasonable effectiveness of deep features as a perceptual metric. In *Proceedings of the IEEE conference on computer vision and pattern recognition*, pages 586–595, 2018.

[49] Junhao Zhuang, Yanhong Zeng, Wenran Liu, Chun Yuan, and Kai Chen. A task is worth one word: Learning with task prompts for high-quality versatile image inpainting. *arXiv preprint arXiv:2312.03594*, 2023.

NeurIPS Paper Checklist

1. **Claims**

   Question: Do the main claims made in the abstract and introduction accurately reflect the paper's contributions and scope?

   Answer: [Yes]

   Justification: We confirm the main claims reflect the paper's contributions and scope.

   Guidelines:

   - The answer NA means that the abstract and introduction do not include the claims made in the paper.
   - The abstract and/or introduction should clearly state the claims made, including the contributions made in the paper and important assumptions and limitations. A No or NA answer to this question will not be perceived well by the reviewers.
   - The claims made should match theoretical and experimental results, and reflect how much the results can be expected to generalize to other settings.
   - It is fine to include aspirational goals as motivation as long as it is clear that these goals are not attained by the paper.

2. **Limitations**

   Question: Does the paper discuss the limitations of the work performed by the authors?

   Answer: [Yes]

   Justification: The paper have conducted a discussion of limiations in the Appendix.

   Guidelines:

   - The answer NA means that the paper has no limitation while the answer No means that the paper has limitations, but those are not discussed in the paper.
   - The authors are encouraged to create a separate "Limitations" section in their paper.
   - The paper should point out any strong assumptions and how robust the results are to violations of these assumptions (e.g., independence assumptions, noiseless settings, model well-specification, asymptotic approximations only holding locally). The authors should reflect on how these assumptions might be violated in practice and what the implications would be.
   - The authors should reflect on the scope of the claims made, e.g., if the approach was only tested on a few datasets or with a few runs. In general, empirical results often depend on implicit assumptions, which should be articulated.
   - The authors should reflect on the factors that influence the performance of the approach. For example, a facial recognition algorithm may perform poorly when image resolution is low or images are taken in low lighting. Or a speech-to-text system might not be used reliably to provide closed captions for online lectures because it fails to handle technical jargon.
   - The authors should discuss the computational efficiency of the proposed algorithms and how they scale with dataset size.
   - If applicable, the authors should discuss possible limitations of their approach to address problems of privacy and fairness.
   - While the authors might fear that complete honesty about limitations might be used by reviewers as grounds for rejection, a worse outcome might be that reviewers discover limitations that aren't acknowledged in the paper. The authors should use their best judgment and recognize that individual actions in favor of transparency play an important role in developing norms that preserve the integrity of the community. Reviewers will be specifically instructed to not penalize honesty concerning limitations.

3. **Theory assumptions and proofs**

   Question: For each theoretical result, does the paper provide the full set of assumptions and a complete (and correct) proof?

   Answer: [NA]

Justification: We did not include theoretical results in our paper.

Guidelines:

- The answer NA means that the paper does not include theoretical results.
- All the theorems, formulas, and proofs in the paper should be numbered and cross-referenced.
- All assumptions should be clearly stated or referenced in the statement of any theorems.
- The proofs can either appear in the main paper or the supplemental material, but if they appear in the supplemental material, the authors are encouraged to provide a short proof sketch to provide intuition.
- Inversely, any informal proof provided in the core of the paper should be complemented by formal proofs provided in appendix or supplemental material.
- Theorems and Lemmas that the proof relies upon should be properly referenced.

4. **Experimental result reproducibility**

   Question: Does the paper fully disclose all the information needed to reproduce the main experimental results of the paper to the extent that it affects the main claims and/or conclusions of the paper (regardless of whether the code and data are provided or not)?

   Answer: [Yes]

   Justification: We have described the model details in the implementation details in Sec.3.1 and carefully described the experimental metrics in the experimental chapter. The information we provide is sufficient and detailed for replication purposes.

   Guidelines:

   - The answer NA means that the paper does not include experiments.
   - If the paper includes experiments, a No answer to this question will not be perceived well by the reviewers: Making the paper reproducible is important, regardless of whether the code and data are provided or not.
   - If the contribution is a dataset and/or model, the authors should describe the steps taken to make their results reproducible or verifiable.
   - Depending on the contribution, reproducibility can be accomplished in various ways. For example, if the contribution is a novel architecture, describing the architecture fully might suffice, or if the contribution is a specific model and empirical evaluation, it may be necessary to either make it possible for others to replicate the model with the same dataset, or provide access to the model. In general. releasing code and data is often one good way to accomplish this, but reproducibility can also be provided via detailed instructions for how to replicate the results, access to a hosted model (e.g., in the case of a large language model), releasing of a model checkpoint, or other means that are appropriate to the research performed.
   - While NeurIPS does not require releasing code, the conference does require all submissions to provide some reasonable avenue for reproducibility, which may depend on the nature of the contribution. For example
     (a) If the contribution is primarily a new algorithm, the paper should make it clear how to reproduce that algorithm.
     (b) If the contribution is primarily a new model architecture, the paper should describe the architecture clearly and fully.
     (c) If the contribution is a new model (e.g., a large language model), then there should either be a way to access this model for reproducing the results or a way to reproduce the model (e.g., with an open-source dataset or instructions for how to construct the dataset).
     (d) We recognize that reproducibility may be tricky in some cases, in which case authors are welcome to describe the particular way they provide for reproducibility. In the case of closed-source models, it may be that access to the model is limited in some way (e.g., to registered users), but it should be possible for other researchers to have some path to reproducing or verifying the results.

5. **Open access to data and code**

Question: Does the paper provide open access to the data and code, with sufficient instructions to faithfully reproduce the main experimental results, as described in supplemental material?

Answer: [Yes]

Justification: We make a detailed description of the implementation details to ensure that they are repeatable and use publicly available text-guided image inpainting datasets. We provide our code in the Appendix.

Guidelines:

- The answer NA means that paper does not include experiments requiring code.
- Please see the NeurIPS code and data submission guidelines (`https://nips.cc/public/guides/CodeSubmissionPolicy`) for more details.
- While we encourage the release of code and data, we understand that this might not be possible, so "No" is an acceptable answer. Papers cannot be rejected simply for not including code, unless this is central to the contribution (e.g., for a new open-source benchmark).
- The instructions should contain the exact command and environment needed to run to reproduce the results. See the NeurIPS code and data submission guidelines (`https://nips.cc/public/guides/CodeSubmissionPolicy`) for more details.
- The authors should provide instructions on data access and preparation, including how to access the raw data, preprocessed data, intermediate data, and generated data, etc.
- The authors should provide scripts to reproduce all experimental results for the new proposed method and baselines. If only a subset of experiments are reproducible, they should state which ones are omitted from the script and why.
- At submission time, to preserve anonymity, the authors should release anonymized versions (if applicable).
- Providing as much information as possible in supplemental material (appended to the paper) is recommended, but including URLs to data and code is permitted.

6. **Experimental setting/details**

   Question: Does the paper specify all the training and test details (e.g., data splits, hyperparameters, how they were chosen, type of optimizer, etc.) necessary to understand the results?

   Answer: [Yes]

   Justification: We have carried out a detailed narration in the implementation details in Sec.3.1.

   Guidelines:

   - The answer NA means that the paper does not include experiments.
   - The experimental setting should be presented in the core of the paper to a level of detail that is necessary to appreciate the results and make sense of them.
   - The full details can be provided either with the code, in appendix, or as supplemental material.

7. **Experiment statistical significance**

   Question: Does the paper report error bars suitably and correctly defined or other appropriate information about the statistical significance of the experiments?

   Answer: [NA] .

   Justification: Based on our experimental experience, the reproducibility of the experiments involved in this work is high, with results that are replicable and stable, rather than simply reporting the highest outcomes. Additionally, previous related work [12, 49, 47, 1, 25] has also not reported error bars. We thus do not run the statistical significance test.

   Guidelines:

   - The answer NA means that the paper does not include experiments.
   - The authors should answer "Yes" if the results are accompanied by error bars, confidence intervals, or statistical significance tests, at least for the experiments that support the main claims of the paper.

- The factors of variability that the error bars are capturing should be clearly stated (for example, train/test split, initialization, random drawing of some parameter, or overall run with given experimental conditions).
- The method for calculating the error bars should be explained (closed form formula, call to a library function, bootstrap, etc.)
- The assumptions made should be given (e.g., Normally distributed errors).
- It should be clear whether the error bar is the standard deviation or the standard error of the mean.
- It is OK to report 1-sigma error bars, but one should state it. The authors should preferably report a 2-sigma error bar than state that they have a 96% CI, if the hypothesis of Normality of errors is not verified.
- For asymmetric distributions, the authors should be careful not to show in tables or figures symmetric error bars that would yield results that are out of range (e.g. negative error rates).
- If error bars are reported in tables or plots, The authors should explain in the text how they were calculated and reference the corresponding figures or tables in the text.

8. **Experiments compute resources**

   Question: For each experiment, does the paper provide sufficient information on the computer resources (type of compute workers, memory, time of execution) needed to reproduce the experiments?

   Answer: [Yes]

   Justification: We state this detailed information of computer resources in Sec.3.1.

   Guidelines:

   - The answer NA means that the paper does not include experiments.
   - The paper should indicate the type of compute workers CPU or GPU, internal cluster, or cloud provider, including relevant memory and storage.
   - The paper should provide the amount of compute required for each of the individual experimental runs as well as estimate the total compute.
   - The paper should disclose whether the full research project required more compute than the experiments reported in the paper (e.g., preliminary or failed experiments that didn't make it into the paper).

9. **Code of ethics**

   Question: Does the research conducted in the paper conform, in every respect, with the NeurIPS Code of Ethics `https://neurips.cc/public/EthicsGuidelines`?

   Answer: [Yes]

   Justification: We confirm that the research involved in the article complies with the NeurIPS Code of Ethics in all respects.

   Guidelines:

   - The answer NA means that the authors have not reviewed the NeurIPS Code of Ethics.
   - If the authors answer No, they should explain the special circumstances that require a deviation from the Code of Ethics.
   - The authors should make sure to preserve anonymity (e.g., if there is a special consideration due to laws or regulations in their jurisdiction).

10. **Broader impacts**

    Question: Does the paper discuss both potential positive societal impacts and negative societal impacts of the work performed?

    Answer: [Yes]

    Justification: The paper have conducted a discussion of broader impacts in the Appendix.

    Guidelines:

    - The answer NA means that there is no societal impact of the work performed.

- If the authors answer NA or No, they should explain why their work has no societal impact or why the paper does not address societal impact.
- Examples of negative societal impacts include potential malicious or unintended uses (e.g., disinformation, generating fake profiles, surveillance), fairness considerations (e.g., deployment of technologies that could make decisions that unfairly impact specific groups), privacy considerations, and security considerations.
- The conference expects that many papers will be foundational research and not tied to particular applications, let alone deployments. However, if there is a direct path to any negative applications, the authors should point it out. For example, it is legitimate to point out that an improvement in the quality of generative models could be used to generate deepfakes for disinformation. On the other hand, it is not needed to point out that a generic algorithm for optimizing neural networks could enable people to train models that generate Deepfakes faster.
- The authors should consider possible harms that could arise when the technology is being used as intended and functioning correctly, harms that could arise when the technology is being used as intended but gives incorrect results, and harms following from (intentional or unintentional) misuse of the technology.
- If there are negative societal impacts, the authors could also discuss possible mitigation strategies (e.g., gated release of models, providing defenses in addition to attacks, mechanisms for monitoring misuse, mechanisms to monitor how a system learns from feedback over time, improving the efficiency and accessibility of ML).

11. **Safeguards**

    Question: Does the paper describe safeguards that have been put in place for responsible release of data or models that have a high risk for misuse (e.g., pretrained language models, image generators, or scraped datasets)?

    Answer: [NA]

    Justification: We utilize the publicly available text-guided image inpainting dataset [12, 35] and the pretrained generation models Stable Diffusion V1.5, there is no relevant description we will set up safeguards when we release the code of NTN-Diff.

    Guidelines:

    - The answer NA means that the paper poses no such risks.
    - Released models that have a high risk for misuse or dual-use should be released with necessary safeguards to allow for controlled use of the model, for example by requiring that users adhere to usage guidelines or restrictions to access the model or implementing safety filters.
    - Datasets that have been scraped from the Internet could pose safety risks. The authors should describe how they avoided releasing unsafe images.
    - We recognize that providing effective safeguards is challenging, and many papers do not require this, but we encourage authors to take this into account and make a best faith effort.

12. **Licenses for existing assets**

    Question: Are the creators or original owners of assets (e.g., code, data, models), used in the paper, properly credited and are the license and terms of use explicitly mentioned and properly respected?

    Answer: [Yes]

    Justification: We utilize the publicly available text-guided image inpainting dataset [12, 35] and the pretrained generation models Stable Diffusion V1.5, both of them state the dataset and model license.

    Guidelines:

    - The answer NA means that the paper does not use existing assets.
    - The authors should cite the original paper that produced the code package or dataset.
    - The authors should state which version of the asset is used and, if possible, include a URL.

- The name of the license (e.g., CC-BY 4.0) should be included for each asset.
- For scraped data from a particular source (e.g., website), the copyright and terms of service of that source should be provided.
- If assets are released, the license, copyright information, and terms of use in the package should be provided. For popular datasets, `paperswithcode.com/datasets` has curated licenses for some datasets. Their licensing guide can help determine the license of a dataset.
- For existing datasets that are re-packaged, both the original license and the license of the derived asset (if it has changed) should be provided.
- If this information is not available online, the authors are encouraged to reach out to the asset's creators.

13. **New assets**

    Question: Are new assets introduced in the paper well documented and is the documentation provided alongside the assets?

    Answer: [NA]

    Justification: We do not introduce new assets in the paper.

    Guidelines:

    - The answer NA means that the paper does not release new assets.
    - Researchers should communicate the details of the dataset/code/model as part of their submissions via structured templates. This includes details about training, license, limitations, etc.
    - The paper should discuss whether and how consent was obtained from people whose asset is used.
    - At submission time, remember to anonymize your assets (if applicable). You can either create an anonymized URL or include an anonymized zip file.

14. **Crowdsourcing and research with human subjects**

    Question: For crowdsourcing experiments and research with human subjects, does the paper include the full text of instructions given to participants and screenshots, if applicable, as well as details about compensation (if any)?

    Answer: [NA]

    Justification: The paper does not involve crowdsourcing nor research with human subjects.

    Guidelines:

    - The answer NA means that the paper does not involve crowdsourcing nor research with human subjects.
    - Including this information in the supplemental material is fine, but if the main contribution of the paper involves human subjects, then as much detail as possible should be included in the main paper.
    - According to the NeurIPS Code of Ethics, workers involved in data collection, curation, or other labor should be paid at least the minimum wage in the country of the data collector.

15. **Institutional review board (IRB) approvals or equivalent for research with human subjects**

    Question: Does the paper describe potential risks incurred by study participants, whether such risks were disclosed to the subjects, and whether Institutional Review Board (IRB) approvals (or an equivalent approval/review based on the requirements of your country or institution) were obtained?

    Answer: [NA]

    Justification: The paper does not involve crowdsourcing nor research with human subjects.

    Guidelines:

    - The answer NA means that the paper does not involve crowdsourcing nor research with human subjects.

- Depending on the country in which research is conducted, IRB approval (or equivalent) may be required for any human subjects research. If you obtained IRB approval, you should clearly state this in the paper.
- We recognize that the procedures for this may vary significantly between institutions and locations, and we expect authors to adhere to the NeurIPS Code of Ethics and the guidelines for their institution.
- For initial submissions, do not include any information that would break anonymity (if applicable), such as the institution conducting the review.

16. **Declaration of LLM usage**

    Question: Does the paper describe the usage of LLMs if it is an important, original, or non-standard component of the core methods in this research? Note that if the LLM is used only for writing, editing, or formatting purposes and does not impact the core methodology, scientific rigorousness, or originality of the research, declaration is not required.

    Answer: [NA]

    Justification: The paper does not involve LLM as any important, original, or non-standard components.

    Guidelines:

    - The answer NA means that the core method development in this research does not involve LLMs as any important, original, or non-standard components.
    - Please refer to our LLM policy (`https://neurips.cc/Conferences/2025/LLM`) for what should or should not be described.

Appendix Overview

Due to page limitation of the mainbody, as indicated by our submission, the supplementary material offers further discussion on the motivation of mid-frequency band and more visual results with higher resolution, which are summarized below:

- More analysis of the high-and-low frequency components in the denoising process, as mentioned in Sec.1 of the mainbody (Sec.A)
- More *intuitions* on hybrid frequency aware diffusion models to text-guided image inpainting, as mentioned in Sec.2.2 of the mainbody (Sec.B)
- The algorithm of NTN-Diff, as mentioned in Sec.2.4 of the mainbody (Sec.C)
- More analysis of computational efficiency for the comparison with state-of-the-arts, as mentioned in Sec.3.2 of the mainbody (Sec.D).
- Additional quantitative results and qualitative analysis with *higher resolution* for the comparison with state-of-the-arts, as mentioned in Sec.3.2 of the mainbody (Sec.E).
- More ablation studies on the impact of text and null-text prompts on low-and-mid frequency bands during denoising process, as mentioned in Sec.3.3.1 of the mainbody (Sec.F).
- Additional generation results for the ablation study about hyperparameter sensitivity analysis of λ for the length of the early and late stage, as mentioned in Sec.3.3.2 of the mainbody (Sec.G).
- We list the limitations and broader impacts (Sec.H).

A More Analysis of the High-and-Low Frequency Components in the Denoising Process

Due to the page limitation, we further conduct experiments to verify the conclusion stated in **Sec. 1 of the mainbody**: *"the low-frequency band fluctuates more significantly during the early stage of the denoising process with high-level noise than the mid- and high-frequency bands."* This observation aligns with the common understanding that diffusion models first recover low-frequency components and progressively refine mid- and high-frequency details. Motivated by this, we experimentally validate the denoising process using several metrics to measure variations in the low-and-high frequency bands at different timesteps, as reported in Table. 4.

We adopt two groups of metrics to analyze the frequency behavior during the denoising process:

- **Low-frequency information:** We adopt *Mean Gray*, *Mean HSV-V*, and *Mean Luma*, which primarily capture the global brightness and luminance structure of the denoised image. These metrics evaluate how well the low-frequency bands are maintained throughout the denoising process.
- **High-frequency information:** We use *Average Gradient*, *Variance*, and *LBP Variance*, which are sensitive to edge sharpness, local contrast, and texture complexity, respectively. These metrics reflect the preservation and recovery of fine details during denoising.

The results show that low-frequency metrics (*Mean Gray*, *HSV-V*, *Luma*) remain nearly unchanged from the beginning, indicating early stabilization. In contrast, high-frequency metrics (*Avg Gradient*, *Variance*, *LBP Variance*) increase steadily in the later timesteps, **confirming that high-frequency details are refined gradually during denoising**, which is consistent with the statement in **Sec. 1 of the mainbody**.

B More Intuition on Hybrid Frequency Aware Diffusion Models to Text-Guided Image Inpainting

Due to page limitation, we offer more visual results of the mid-frequency band of the denoising process. Fig.8(a) illustrates the text-guided denoising results for mid-frequency band. To validate its stability, we visualize the layout information as bounding box for each step, which, as indicated

Table 4: Metrics measuring the low-and-high frequency band variations during the denoising process, confirming that diffusion models typically recover the low-frequency band first and progressively refine the mid-and-high frequency bands.

Timesteps	Mean Gray	Mean HSV-V	Mean Luma	Avg Gradient	Variance	LBP Variance
0	**120.9**	**136.0**	**120.9**	**59.01**	**3955.0**	**4.45**
5	120.8	134.6	120.8	75.07	4098.3	3.71
10	120.7	133.5	120.7	101.58	4378.9	3.25
15	120.7	133.7	120.7	133.26	4790.8	3.07
20	120.9	135.1	120.9	164.23	5274.8	3.07
25	121.2	137.3	121.2	190.49	5743.9	3.15
30	121.4	139.2	121.4	209.84	6099.5	3.25
35	121.1	140.0	121.1	222.03	6291.1	3.32
40	120.5	140.1	120.5	228.75	6363.9	3.35
45	119.9	139.8	119.9	232.19	6394.8	3.38
50	119.5	139.5	119.5	233.88	6419.5	3.40

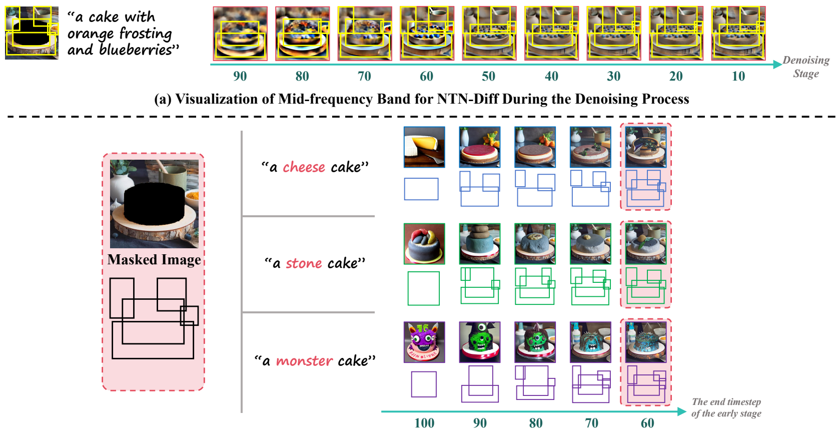

(a) Visualization of Mid-frequency Band for NTN-Diff During the Denoising Process

(b) More Results on Mid-frequency Band for NTN-Diff During the Denoising Process

Figure 8: We investigate the text-guided denoising process for the mid-frequency bands. For each step, we employ the bounding boxes to visualize the variations for layout information in (a) and the changes of layout information for the same image based on three similar text prompts. the denoised mid-frequency band changes during the initial early stage owing to text prompts with high-level noise, yet quickly converges by the end of the early stage, which further leads to the stable states with nearly no influence by text prompt across the whole late stage.

by [5, 6, 43], is closely related to the mid-frequency band. The denoised mid-frequency band also changes during the initial early stage owing to text prompts with high-level noise, yet quickly converges by the end of the early stage e.g., 60-th step, which further leads to the stable mid-frequency band with *nearly* no influence by text prompt across the whole late stage with low-level noise. We further exhibit additional visual results by performing the experiments on the same image based on three similar text prompts. Despite the different text prompts, the mid-frequency can quickly converge by the end of the early stage, *e.g.*, 60-th. Following the above, we propose to exploit the mid-frequency band during denoising process, which plays the pivotal role of achieving the semantics consistency upon text prompts, while can better achieve the semantics consistency between masked and unmasked regions, to further preserve its own frequency band well, owing to its robustness to the text prompt during the denoising process.

C The Algorithm of NTN-Diff

Our proposed NTN-Diff pipeline consists of a *null-text denoising process* (Sec. 2.3.1) that avoids the influence of text prompts, and a *text-guided denoising process* (Sec. 2.3.2) that reconstructs the masked regions while replacing the low-frequency band of its denoised output with that from the null-text denoising process. Building upon this design, we further utilize the denoised mid-frequency information to guide another *null-text denoising process* (Sec. 2.3.3) by substituting the mid-frequency band accordingly. In addition, a late-stage *text-guided denoising process* (Sec. 2.4) is conducted, during which the unmasked regions from the early stage of the diffusion process are progressively substituted to preserve structural consistency. Based on the above, we summarize the complete algorithm of our proposed *null-text-null frequency-aware diffusion model* in Algorithm 1 below:

Algorithm 1 NTN-Diff

```
Input: masked image $I$, binary mask $M$, text prompt $C$, null-text prompt $C_\emptyset$
Output: inpainted image $I'$

I. Diffusion Process for Unmasked Regions
Extract the initial latent feature of the unmasked region $z_0^{gt} = E(I)$.
for $t = 0$ to $T_{inv} - 1$ do
    Compute $z_{t+1}^{gt}$ from $z_t^{gt}$;
end for{DDIM inversion}

II. Early Stage
Initialize $z_T^{un}$, $z_T^{text}$, $z_T^{in} \sim \mathcal{N}(0, 1)$.
for $t = T$ to $\lambda T + 1$ do
    Substitute the unmasked regions of $z_t^{un}$ with the corresponding counterpart of $z_t^{gt}$ via Eq.3;
    Compute $z_{t-1}^{un}$ from $z_t^{un}$, conditioned on $C_\emptyset$ via Eq.4;
    Substitute low-frequency band of $z_t^{text}$ with the corresponding counterpart of $z_t^{un}$ via Eq.5–7;
    Compute $z_{t-1}^{text}$ from $z_t^{text}$, conditioned on $C$;
    Substitute mid-frequency band of $z_t^{in}$ with the corresponding counterpart of $z_t^{text}$ via Eq.8–10;
    Compute $z_{t-1}^{in}$ from $z_t^{in}$, conditioned on $C_\emptyset$;
end for

III. Late Stage
for $t = \lambda T$ to $1$ do
    Substitute unmasked regions of $z_t^{in}$ with the corresponding counterpart of $z_t^{gt}$ via Eq.11;
    Compute $z_{t-1}^{in}$ from $z_t^{in}$, conditioned on $C$;
end for
Output the final inpainted image $I' = D(z_0^{in})$.
```

D More Analysis of Computational Efficiency in the Sec.3.2 of the Mainbody

As indiacted in the mainbody, we further provide the inference time and VRAM consumption of our proposed NTN-Diff model, and compared it with several representative baselines, which are reported in Table. 5. Our inference time is comparable to **BrushNet** [12] and faster than recent methods such as **HDP** [25] and **PP** [49]. Moreover, our model consumes less VRAM than other text-guided inpainting models, **owing to the fact that our method performs low- and mid-frequency substitution across different branches after each denoising step**. The key idea is that, being decoupled from the resource-intensive denoising process itself, our approach introduces only negligible additional memory cost compared to the single denoising process in **BLD** [1].

Table 5: Inference time and VRAM consumption comparison among different models. NTN-Diff achieves a comparable inference time while exhibiting the lowest memory cost among all methods.

Methods (Venue)	**Inference Time (s)** ↓	**VRAM Consumption (GB)** ↓
BLD [1] (TOG'23)	**4.78**	**2.11**
PP [49] (ECCV'24)	7.24	4.09
BrushNet [12] (ECCV'24)	6.59	3.19
HDP [25] (ICLR'25)	10.57	11.75
NTN-Diff (Ours)	6.96	**2.11**

Table 6: Quantitative comparisons between NTN-Diff* and other diffusion-based inpainting models over EditBench for inpainting are shown, where all models use Stable Diffusion V1.5 as the baseline model. **red** and **blue** stand for the best and second best result. NTN-Diff* achieves the best result.

Metrics		**Masked Region Preservation**				**Text Alignment**
Models	**Venue**	**PSNR**↑	**MSE**$_{\times 10^3}$↓	**LPIPS**$_{\times 10^3}$↓	**SSIM**$_{\times 10^2}$↑	**CLIP Score**↑
SDI [32]	CVPR' 22	23.25	6.94	24.30	90.13	28.00
BLD [1]	TOG' 23	20.89	10.93	31.90	85.09	28.62
CNI [47]	ICCV' 23	12.71	69.42	159.71	79.16	28.16
CNI* [47]	ICCV' 23	22.61	35.93	26.14	94.05	27.74
PP [49]	ECCV' 24	23.34	20.12	24.12	91.49	27.80
BrushNet* [12]	ECCV' 24	**33.66**	**0.63**	10.12	98.13	28.87
BrushEdit* [17]	ArXiv' 24	32.97	0.70	**7.24**	**98.60**	**29.62**
HDP [25]	ICLR' 25	23.07	6.70	24.32	92.56	28.34
NTN-Diff* (Ours)	-	**36.83**	**0.28**	**5.39**	**99.46**	**29.72**

* with blending operation of BrushNet

E Additional Quantitative and Qualitative analysis in the Sec.3.2 of the Mainbody

Evaluation metric. We adopt five metrics to evaluate the inpainted results below: Peak Signal-to-Noise Ratio (**PSNR**), structural similarity index (**SSIM**) [37] and Mean Squared Error (**MSE**) evaluate low-level pixel-wise differences between generated images and their ground truth counterparts. Additionally, Learned Perceptual Image Patch Similarity (**LPIPS**) [48] measures perceptual similarity by computing the distance between deep features extracted from a pre-trained neural network, offering a robust metric for assessing perceptual alignment; CLIP Similarity (**CLIP Score**) [38] measures text-image consistency by projecting both the generated images and their corresponding text prompts into a shared embedding space using the CLIP model. It then evaluates the similarity between their embeddings.

As indiacted in the mainbody, we further exhibit additional quantitative results by performing the experiments on the EditBench [35]; see Table.6. It is observed that **NTN-Diff** enjoys larger PSNR, SSIM and CLIP Score, together with smaller MSE and LPIPS than the competitors. Notably, **BrushEdit**[17] remains the large performance margins (at most, 3.86% for PSNR, 0.42% for MSE 1.85% for LPIPS, 0.86% for SSIM, and 0.1% for CLIP Score) compared to **NTN-Diff** in Table.6. We also present the quantitative results of **NTN-Diff** with the pixel-level blending operation of [12], named **NTN-Diff***, to preserve the unmasked regions, which demonstrates the ability to tame the hybrid frequency issue, the results further verifies the intuition in Sec.1 of the mainbody – *NTN-Diff can achieve the semantics consistency between mid-and-low frequency bands across masked and unmasked regions, while preserving unmasked regions.*

To shed more light on the advantages of our method, we further perform the visual analysis on the inpainted results with *the higher resolution*. Fig.9 delivers the following: due to the discrepancy between the diffusion process for unmasked regions substitution and the denoising process for masked region alignment upon text prompt. BLD [1] inevitably generate the content out of the masked regions (the first column of the Fig.9(a)). Note that, PP [49] and BrushNet [12] often exhibits the unreasonable inpainted result, *e.g.*, The extra woman(the 4th row of PP in Fig.9(a)) and the disappeared dinosaur (the 1st row of BrushNet in Fig.9(b)), owing to the unmasked regions are disrupted, thus fails to reconstruct the masked region as per text prompt, which attributes to the fact that *the low-frequency bands for both masked and unmasked regions are easily to be changed by text prompts, especially under the early stage of the text-guided denoising process with high-level noise. As opposed to that, mid-frequency band can better achieve the semantics consistency between masked and unmasked regions, while preserve its own frequency band well, than low-frequency band, owing to its robustness to the text prompt during the denoising process, while the previous arts fail to disentangle all frequency bands during the denoising process especially for its early stage with high-level noise* (see Sec.1 of the mainbody).

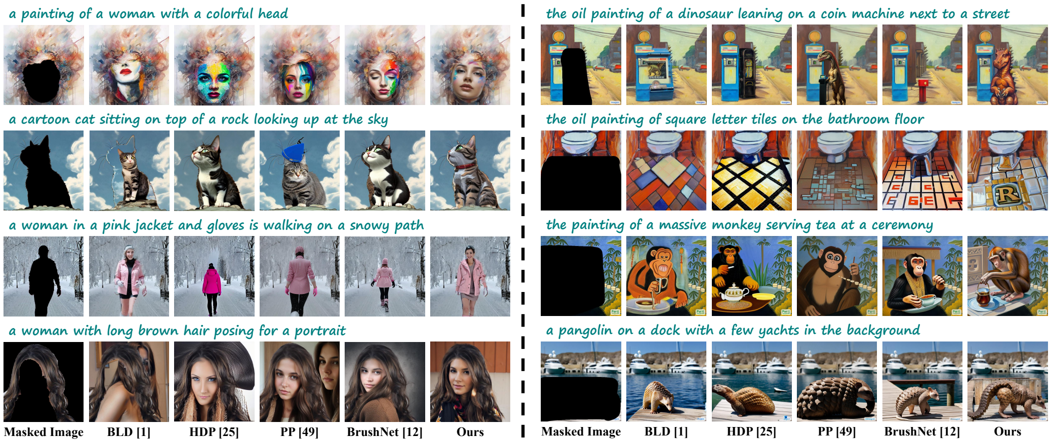
a painting of a woman with a colorful head
a cartoon cat sitting on top of a rock looking up at the sky
a woman in a pink jacket and gloves is walking on a snowy path
a woman with long brown hair posing for a portrait
the oil painting of a dinosaur leaning on a coin machine next to a street
the oil painting of square letter tiles on the bathroom floor
the painting of a massive monkey serving tea at a ceremony
a pangolin on a dock with a few yachts in the background
Masked Image
BLD [1]
HDP [25]
PP [49]
BrushNet [12]
Ours
Masked Image
BLD [1]
HDP [25]
PP [49]
BrushNet [12]
Ours

(a) BrushBench

(b) EditBench

Figure 9: Comparison of the text-guided inpainted results with the state-of-the-arts on BrushBench [12] and EditBench [35]. NTN-Diff delivers the superior inpainted results over others, which can simultaneously preserve the unmasked regions while achieve the semantics consistency between unmasked and inpainted masked regions.

Table 7: Ablation studies on the impact of text and null-text prompts on low-and-mid frequency bands during denoising process: TTN-Diff, NTT-Diff and TTT-Diff for the early stage, based on the same text-guided denoising process (Sec.2.4 of the mainbody) for the late stage. **red** and **blue** stand for the best and second best result.

Dataset	Metric	TTN-Diff	NTT-Diff	TTT-Diff	Ours(NTN-Diff)
EditBench	**IR**$_{\times 10}$↑	1.57	**2.12**	1.34	**3.10**
	PSNR↑	22.57	**22.58**	22.51	**22.65**
	LPIPS$_{\times 10^3}$↓	25.12	**24.99**	25.24	**24.21**
	CLIP Score↑	28.87	**28.89**	28.81	**28.95**
BrushBench	**IR**$_{\times 10}$↑	9.61	**10.32**	9.22	**11.12**
	PSNR↑	28.06	**28.08**	28.01	**28.10**
	LPIPS$_{\times 10^3}$↓	44.63	**44.55**	44.88	**44.09**
	CLIP Score↑	25.94	**25.97**	25.89	**26.09**

F More Ablation Studies on the Impact of Text and Null-Text Prompts on Low-and-Mid Frequency Bands during Denoising Process

As mentioned in Sec.3.3.1 of the mainbody, due to page limitation, we further provide more ablation studies on the impact of text and null-text prompts on low-and-mid frequency bands during denoising process on BrushBench and EditBench datasets with three variants: **TTN-Diff**: replacing the first null-text denoising process with the text-guided denoising process; **NTT-Diff**: replacing the last null-text denoising process with the text-guided denoising process; **TTT-Diff**: replacing both the first and last null-text denoising processes with the text-guided denoising processes; Table.7 suggests that our **NTN-Diff** outperforms **NTT-Diff**, despite the denoised mid-frequency band well aligns with the text prompts especially for masked regions, while also encodes the information related to low-frequency band from the first null-text denoising process, which verifies that *the last null-text denoising process can achieve semantics consistency between mid-and-low frequency bands across masked and unmasked regions, by denoising the low-frequency band throughout the path to be semantically consistent to mid-frequency band, with no influence from text prompts*, which is in line with Sec.2.3.3 of the mainbody; **TTN-Diff** exhibits a substantial performance degradation, confirming that *the null-text denoising process conditioned on null-text prompt can avoid being influenced by text prompts even under the high-level noise, focusing primarily on low-frequency band,* hence validating the important the first null-text denoising process (Sec.2.3.1 of the mainbody). We illustrate the above intuitions in Fig.10.

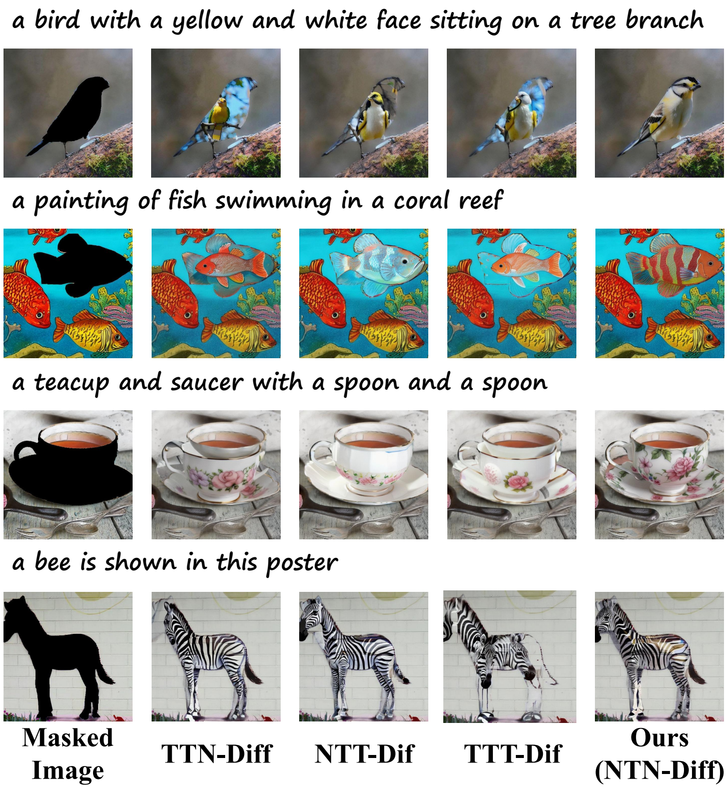
a bird with a yellow and white face sitting on a tree branch
a painting of fish swimming in a coral reef
a teacup and saucer with a spoon and a spoon
a bee is shown in this poster
Masked Image
TTN-Diff
NTT-Dif
TTT-Dif
Ours (NTN-Diff)

Figure 10: The inpainted output about the impact of text and null-text prompts on low-and-mid frequency bands during denoising process, with the first null-text denoising process (Sec.2.3.1 of the mainbody), the second text-guided denoising process (Sec.2.3.2 of the mainbody) and the last null-text denoising process (Sec.2.3.3 of the mainbody), NTN-Diff can achieve the better inpainted results than others.

G Additional Generation Results for the Ablation Study in Sec.3.3.2 of the mainbody

As mentioned in Sec.3.3.2 of the mainbody, due to page limitation, we further provide more visual results to analyse the parameter λ in the denoising process (Sec.2.2 of the mainbody), which is utilized to divide the denoising process into *early* and *late* stages, demarcated by the critical step λT. see Fig.11. When $\lambda = 0.9$, the performance is the worst with the shortest early stage, such as blue background in the 4th row. When $\lambda = 0.6$ with the balance of early and late stage, the best performance of image quality, unmasked region preservation and text alignment are achieved, such as the face of the cat in the first rows, confirming the rational that *the denoised low-frequency band for the masked regions is guided by the denoised mid-frequency band within the whole early stage, which is guided by text prompts for a few number of steps from text-guided late denoising process to avoid the large influence from text prompts to be inconsistent for unmasked regions, thus the desirable length of early stage can make the low-frequency band under the mid-frequency guidance for masked regions achieve the consistency to the substituted unmasked regions for ground truth*, which is consistent to Sec.2.4 of the mainbody.

H Limitations and Broader Impacts

Limitations. Unlike previous state-of-the-art methods that fine-tune Stable Diffusion (v1.5) on large-scale datasets for text-guided image inpainting, which typically require extensive time and computational resources for training, our method introduces a plug-and-play frequency-aware null-text-null diffusion framework. This framework substitutes mid-and-low frequency bands during the

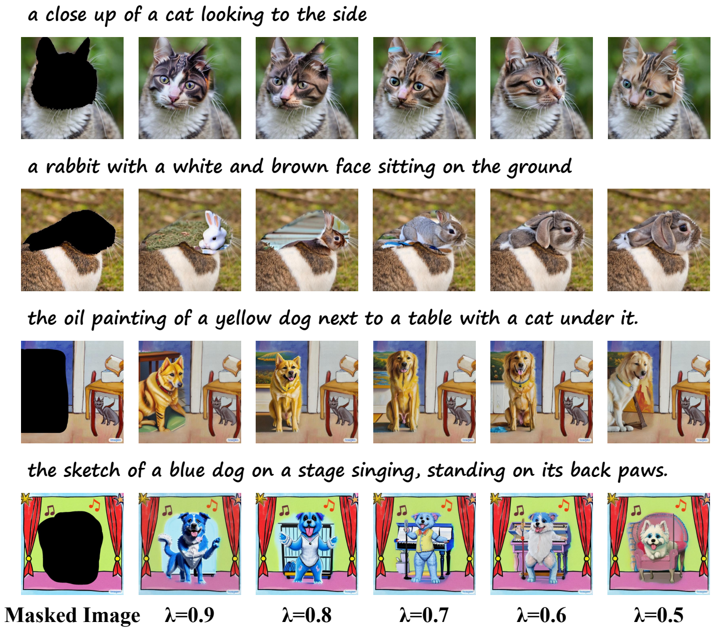
a close up of a cat looking to the side
a rabbit with a white and brown face sitting on the ground
the oil painting of a yellow dog next to a table with a cat under it.
the sketch of a blue dog on a stage singing, standing on its back paws.
Masked Image
λ=0.9
λ=0.8
λ=0.7
λ=0.6
λ=0.5

Figure 11: The inpainted output about hyperparameter sensitivity analysis of λ for the length of the early and late stage, when $\lambda = 0.6$ with the balance of early and late stage, NTN-Diff can achieve the better inpainted results than others.

early stage of the denoising process and, as a result, involves three parallel null-text-null denoising processes in the early stage, resulting in a larger computational cost than single process. Nevertheless, it shares the same order of magnitude as the previous methods.

Broader Impacts. Our NTN-Diff can achieve the masked regions to be generated according to the text prompt, while preserve the unmasked regions, our method may raise certain ethical concerns. The inpainted image could potentially be misused in the creation of misleading information. We strongly advocate for the establishment of clear accountability in the use of such technologies, along with enhanced legal and technical oversight, to ensure they are applied responsibly.